Automatika

Journal for Control, Measurement, Electronics, Computing and Communications

ISSN: 0005-1144 (Print) 1848-3380 (Online) Journal homepage: https://www.tandfonline.com/loi/taut20

PSO Based reduced order modelling of autonomous AC microgrid considering state perturbation

Mudita Juneja, S. K. Nagar & Soumya R. Mohanty

To cite this article: Mudita Juneja, S. K. Nagar & Soumya R. Mohanty (2020) PSO Based reduced order modelling of autonomous AC microgrid considering state perturbation, Automatika, 61:1, 66-78, DOI: 10.1080/00051144.2019.1682867

To link to this article: https://doi.org/10.1080/00051144.2019.1682867

Published online: 07 Nov 2019.

AUTOMATIKA
2020, VOL. 61, NO. 1, 66–78
https://doi.org/10.1080/00051144.2019.1682867

REGULAR PAPER

OPEN ACCESS Check for updates

PSO Based reduced order modelling of autonomous AC microgrid considering state perturbation

Mudita Juneja, S. K. Nagar and Soumya R. Mohanty

Department of Electrical Engineering, Indian Institute of Technology (BHU), Varanasi, India.

ABSTRACT

Reduced order modelling of complex autonomous microgrid system is crucial to its small signal modelling and stability concerns. To reduce the storage requirements and computational time, the order of such microgrids can be reduced by Model Order Reduction (MOR) techniques. This paper presents an optimal reduction technique, which retains dominant poles of the original system and achieves subsequent error minimization through the Particle Swarm Optimization algorithm (PSO). The 36th order complex microgrid system is reduced to 9^{th} order approximant, which retains the significant dynamics of the original system. The simulation results reflect the superiority of the proposed method as compared to the balanced truncation method in terms of the time and frequency domain analysis of the reduced order equivalents. State perturbation in the state space model has also been considered in full as well as reduced order system dynamics and eigenvalue analysis for system stability.

ARTICLE HISTORY
Received 29 October 2018
Accepted 31 July 2019

KEYWORDS
Autonomous microgrid; eigenvalue sensitivity; model order reduction; particle swarm optimization; small signal; state perturbation

1. Introduction

The integration of renewable energy resources to the main grid to meet the load requirements is a viable option with the development of microgrid system. A microgrid is an interconnection of several Distributed Energy Resources (DERs) such as photovoltaic, fuel cells, wind turbines, etc., to meet the load demands either in grid-connected mode or autonomous mode. The dependence on exhaustible energy resources and their environmental degradation is easily controlled by increasing utilization of renewable-based microgrids in the main utility grid.

The small signal modelling and performance evaluation of microgrids have become increasingly important because of various reasons. The Phase Locked Loop (PLL) synchronization and interfacing circuitry to connect the equivalent model of Distributed Generators (DGs) sources to ac loads and different buses are crucial. Even the power electronics converter which offers improved power quality and flexibility in control poses threats to system stability due to their low-inertia as compared to other components, causing oscillations manifested due to network dynamics. As a matter of fact, the major concern in the reliable operation of a microgrid is the small-signal stability. Thus it is quite essential to analyze the small-signal model and select different parameters of controller or filter, in order to enhance the system dynamics and ensure power quality within acceptable limits. Another limitation to microgrid small signal analysis is the dimensional complexity due to the diversity of control strategy in DGs and components involved [1]. The system dynamics of each DER in a microgrid system is represented by 15 states [2], offering limited analytical insights. This leads to high computational cost when applied to investigate the dynamics of large microgrids with many inverters. Thus, MOR becomes necessary so as to simplify the model, without compromising much with system dynamics.

Several methods have been explored to reduce the dimensionality of large power systems in the literature [1–8]. Aggregation, balanced realization, truncation, and certain mixed methods have been discussed to reduce the order of these power systems in [3]. Balanced Truncation (BT) technique has been applied to large power systems in [4] using a number of matrix calculations. But the main drawback lies in the frequent occurrence of a steady-state error in BT-reduced order model. Further, reference [5] reduces a ninth order small signal model of the microgrid to its fifth order approximation using singular perturbation and kron method. Due to the presence of two-time scales in AC microgrids, thirty-sixth order microgrid model has been reduced to fifteenth order by singular perturbation method in [6]. In [7], a simplified sixth order islanded microgrid model has been reduced to fourth order by retaining the very fast dynamics in the response through singular perturbation and direct

CONTACT Mudita Juneja mjuneja.rs.eee14@iitbhu.ac.in Department of Electrical Engineering, Indian Institute of Technology (BHU), Varanasi, India 221005.

truncation methods. A three-time scale model was developed for an AC microgrid in [8] based on the relative eigenvalue loci. This droop based inverter interfaced DGs evaluated model parameter ϵ for order reduction of a linearized system based on singular perturbation theory which depends upon the system time constant derived from values of circuit parameters.

On the contrary to the methods adopted in literature for order reduction, a simpler yet equally effective MOR technique proposed in this paper for reduced order modelling of 36th order microgrid system in autonomous mode is Dominant pole technique. This technique preserves the larger time constants in reduced order models by retaining the dominant poles of the system, as the faster dynamics die out early and do not affect the system much [9]. The improvization in the MOR of this system is further achieved by application of the PSO algorithm, in lieu of formulation of an appropriate objective function because of the high flexibility and reduction accuracy. PSO is considered as a strong candidate for optimization objective widely used in various field of engineering [10,11]. It adapts its behaviour from natural biomes by working in groups to achieve a certain performance measure. Thus, the novelty of the proposed technique lies in the amalgamation of these two techniques of dominant pole retention and PSO algorithm, exploited for microgrid systems, which not only simplifies the reduction process but also utilizes the advantages of both the methods [12]. The simplified procedure based on optimization not only results in an adaptive reduced model due to the iterative PSO algorithm but also enhances system robustness which has been proved through the results obtained on perturbed variant of the model. As a matter of fact, the present analysis work greatly reduces the mathematical complexity of a two-inverter microgrid structure from 36th to 9^{th} order model, i.e. the reduction in state space formulation is by 75%. The study of state perturbation caused by various parameter variations, in the small-signal model of microgrids with limited no. of states, is considered in [13] for a low-frequency eigenvalue. The state uncertainty is considered in this work to explore their effects on small signal stability for full order as well as reduced order system. The small changes in eigenvalues have been studied to analyze the frequency and damping changes when the order is to be reduced for accurate analysis under uncertain conditions. Although various MOR techniques are explored for small signal analysis of microgrid configuration, the rigorous and comprehensive analysis for the same is not reported in the earlier literature. Therefore, this paper develops an optimal reduction technique deploying the dominancy characteristics for the higher order microgrid systems. The main contribution of the paper is highlighted below,

- Implementation of MOR in Autonomous Microgrid by dominant pole augmented by PSO by reducing the L_1 error norm.
- Impact of state perturbation to full order as well as reduced order microgrid structure.
- Evaluation of reduction errors subjected to step, ramp and impulse function for full order as well as reduced order systems.
- Calculation of eigenvalue sensitivity as well as various modes associated with the participation factor analysis.

This paper is organized as follows: Part I gives the small signal model of the autonomous system while defining the transfer function model. Part II discusses the optimal model order reduction technique proposed in this work. Part III gives the discussion and results obtained by state perturbations and the optimal reduced order modelling, in comparison to BT technique. Part IV describes the eigenvalue and sensitivity analysis of the full order and reduced order autonomous small signal model. The conclusion at the end highlights the key developments in the paper.

2. System architecture

The autonomous microgrid architecture considered in this work is represented in Figure 1. It consists of two DERs connected to their individual local buses through the LC filter and coupling inductances. The two local buses are coupled through a line of impedance $R_{line}+jXL_{line}$. When the Point of Common Coupling (PCC) is closed, the AC buses are connected to the main utility grid, and hence, the microgrid works in "Grid-tied mode." Whereas, when PCC is open, then the microgrid is cut-off from the main grid and is in "Autonomous mode".

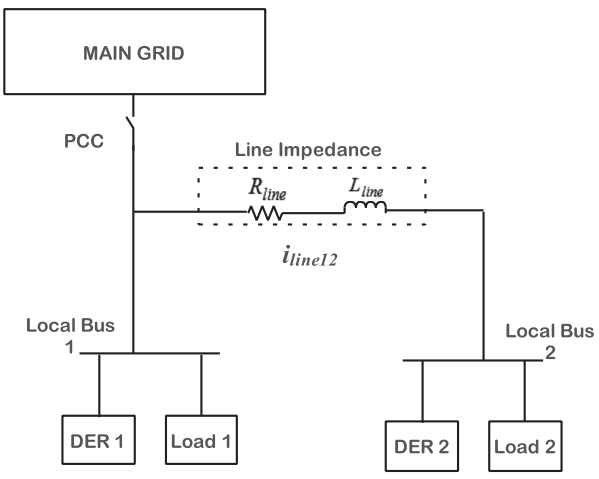

Figure 1. Proposed Microgrid Scheme.

3. Small signal modelling of autonomous microgrid system

Although small signal modelling of Microgrid already exists in the literature [1,2,14–18]; still modelling with the necessary mathematical formulation is done for subsequent MOR analysis, subject to state perturbation for both full order as well as reduced order system. The small signal modelling of the system in Figure 1, requires the state space analysis of the two inverters, loads and line dynamics. Figure 2 shows the block diagram of a DG based inverter. The DG is connected to the load and common bus through a Voltage Source Inverter (VSI). The control strategy is this block diagram is implemented by three control loops: (a) outer power loop, which evaluates the desired frequency and voltage of the inverter through droop control technique; (b) Inner voltage control loop, which gives the reference currents through inductor; (c) Inner current control loop, which evaluates the reference voltages to direct the State Vector Pulse Width Modulation (SVPWM) block to generate signal for the inverter.

The basic idea behind power sharing in the power controller block is to compensate any increase in the load side, in accordance with droop characteristics, through a decrease in the frequency and voltage amplitude of the system [1]. The instantaneous active and reactive powers are calculated from the output currents and voltages. The average powers corresponding to the fundamental component are then obtained by passing these instantaneous powers through low pass filter with cut- off frequency of ω_c.

The reference frequency, ω^r and the reference voltage signal, v_{oq}^r are therefore generated using conventional P-ω and Q-V droop characteristic equations, such that,

$$\omega^r = \omega_n - mP \tag{1}$$

$$v_{oq}^r = V_{oq,n} - nQ \tag{2}$$

where m, n are the static droop gain, ω_n is the nominal frequency, $V_{oq,n}$ is the nominal voltage of q-axis (voltage of d-axis set to zero) and P, Q are the filtered output active and reactive powers.

A dq-based PLL with conventional PI strategy was chosen to measure the frequency of the system. The input signal to the PLL block is the d-axis component of the voltage measured across the filter capacitor. In the voltage control loop, the reference signals obtained from the power controller are compared to the measured angular frequency from the PLL block and measured q axis voltage by using conventional PI controllers. The reference inductor currents generated by voltage controller are compared by their measured values to obtain an error signal which thereby produces a set-point voltage for input to SVPWM block. Reduced Total Harmonic Distortion (THD), simplified DSP implementation and fast processing makes, Space Vector Pulse Width Modulation advantageous over other PWM techniques. It lowers the frequency oscillation and is thus used in these microgrid systems.

The load and line dynamics are referred to in the global reference frame, whereas each inverter is mathematically modelled in its own local frame (d-q). The individual inverter state equations are derived in terms of their individual local reference frame [2]. The input and output quantities of individual inverters can be transformed from their individual frame to a common reference frame (D-Q) using the transformation matrix, $\boldsymbol{T}$ as given in (3). The angle θ, as shown in Figure 3, represents the angle between an individual inverter reference frame and the common global reference frame, which translates electrical quantities from local to a common frame and vice versa.

$$\boldsymbol{T} = \begin{bmatrix} \cos\theta & -\sin\theta \\ \sin\theta & \cos\theta \end{bmatrix} \tag{3}$$

where, $\theta = \int(\omega - \omega_{common})$

Considering the system to be autonomous, i.e. disconnected to the main grid, the phase angle measured by the PLL of inverter 1 can be chosen as the reference for the overall interconnected system. The resultant reference angles calculated for both DERs can be used

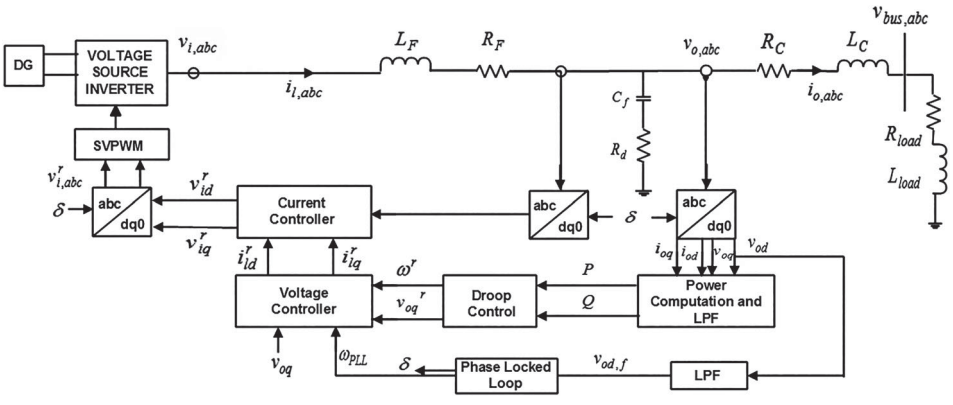

Figure 2. Block Diagram of DG based Inverter.

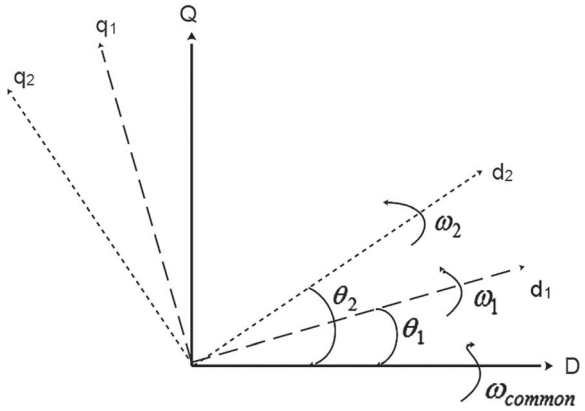

Figure 3. Reference frame Transformation.

as;

$$\dot{\delta}_1 = \omega_{PLL,1} - \omega_{PLL,1} = 0 \tag{4}$$

$$\dot{\delta}_2 = \omega_{PLL,1} - \omega_{PLL,2} \tag{5}$$

where, ω_{PLL1} and ω_{PLL2} are calculated from DER 1 and DER 2, respectively.

4. Microgrid model

4.1. State-space modelling

The first step towards finding the complete state space model of the microgrid system is to determine the Operating point to linearize the non-linear model in its vicinity [19].

Given a non-linear set of state equations, the general form is given as;

$$\dot{x} = f(x,u);\ y = g(x,u) \tag{6}$$

To find the linear equivalent of these non-linear equations, it is desired to evaluate an operating point about which the model can be safely considered as linear. These set of operating points ($x_{0,}$ u_0) are calculated as;

$$\begin{aligned} 0 &= f(\boldsymbol{x}_0, \boldsymbol{u}_0) \\ \boldsymbol{y}_0 &= g(\boldsymbol{x}_0, \boldsymbol{u}_0) \end{aligned} \tag{7}$$

Thereafter, the model is linearized by finding the deviation about the operating point as; $\Delta\boldsymbol{x} = \boldsymbol{x} - \boldsymbol{x}_0$; $\Delta\boldsymbol{u} = \boldsymbol{u} - \boldsymbol{u}_0$; $\Delta\boldsymbol{y} = \boldsymbol{y} - \boldsymbol{y}_0$

The complete small signal modelling of the two inverter architecture as in Figure 1 is achieved by combining the models of the two inverters, x_{inv1} and x_{inv2} respectively, into one state space as given in [1];

$$\begin{aligned} \boldsymbol{x_{inv}}1 = [&\delta_1 P_1 Q_1 \varphi_{d1} \varphi_{q1} \gamma_{d1} \gamma_{q1} i_{ld1} i_{lq1} v_{od1} v_{oq1} \\ &i_{od1} i_{oq1} \varphi_{PLL1} v_{od1,f}] \end{aligned} \tag{8}$$

$$\begin{aligned} \boldsymbol{x_{inv}}2 = [&\delta_2 P_2 Q_2 \varphi_{d2} \varphi_{q2} \gamma_{d2} \gamma_{q2} \\ &i_{ld2} i_{lq2} v_{od2} v_{oq2} i_{od2} i_{oq2} \varphi_{PLL2} v_{od2,f}] \end{aligned} \tag{9}$$

$$\boldsymbol{x_{inv}} = [\boldsymbol{x_{inv}}1 \boldsymbol{x_{inv}}2] \tag{10}$$

where, for both DER, i.e. $i = 1,2$; δ_i is the reference angle of DER i, P_i, Q_i are the filtered output powers, $\varphi_{di}, \varphi_{qi}$ are the state variables from the voltage controller representing an error signal from reference frequency and reference voltage, γ_{di}, γ_{qi} are the state variables from the current controller representing error signal from reference inductor currents in dq axis, i_{ldi}, i_{lqi} are the filter inductor currents in dq axis, v_{odi}, v_{oqi} are the output voltages in dq axis, i_{odi}, i_{oqi} are the output currents in dq axis, $v_{odi,f}$ is the d-axis output voltage filtered through LPF with a corner frequency of $\omega_{C,PLL}$, φ_{PLLi} is the state variable from PLL, given as $\varphi_{PLLi} = -v_{odi,f}$ of DER *i*.

The load and line dynamics of the system are modelled by considering the current through the load capacitances in both the inverters, i.e. $i_{loadDQ1}$ and $i_{loadDQ2}$ and, the current through line capacitance, i.e. $i_{lineDQ21}$ as state variables, given as;

$$\dot{i}_{loadDi} = \frac{1}{L_{load}}(-R_{load} i_{loadDi} + v_{bDi}) + \omega_{PLLi} i_{loadQi} \tag{11}$$

$$\dot{i}_{loadQi} = \frac{1}{L_{load}}(-R_{load} i_{loadQi} + v_{bQi}) - \omega_{PLLi} i_{loadDi} \tag{12}$$

where, $i = 1, 2$; R_{load}, L_{load} are load resistance and inductance respectively.

The collective load model from the two inverters is given as, $\boldsymbol{x_{load}} = [i_{loadD1} i_{loadQ1} i_{loadD2} i_{loadQ2}]$.

$$\begin{aligned} \dot{i}_{lineD21} = &\frac{1}{L_{line}}(-r_{line} i_{lineD} + v_{bD2} - v_{bD1}) \\ &+ \omega_{PLL} i_{lineQ} \end{aligned} \tag{13}$$

$$\begin{aligned} \dot{i}_{lineQ21} = &\frac{1}{L_{line}}(-r_{line} i_{lineQ} + v_{bQ2} - v_{bQ1}) \\ &+ \omega_{PLL} i_{lineD} \end{aligned} \tag{14}$$

where, r_{line}, L_{line} are line resistance and inductance respectively and v_{bDi}, v_{bQi} are bus voltages in common DQ-reference frame.

The line state space contributes two state variables in the overall dynamics given as, $\boldsymbol{x_{line}} = [i_{lineD21} i_{lineQ21}]$.

After linearization of the complete system about a stable operating point as given and rearranging the state variables and output variables in order as in (17), the complete 36th order state space model for the autonomous microgrid system is obtained from (10–14) as;

$$\Delta\dot{\boldsymbol{x}} = \boldsymbol{A}\Delta\boldsymbol{x} + \boldsymbol{B}\Delta\boldsymbol{u} \tag{15}$$

$$\Delta\boldsymbol{y} = \boldsymbol{C}\Delta\boldsymbol{x} \tag{16}$$

Where; $\boldsymbol{A}$ is the state matrix (36×36), $\boldsymbol{B}$ is the input matrix (36×4), and $\boldsymbol{C}$ is the output matrix (6×36)

$$\text{State vector, } \boldsymbol{x} = [\boldsymbol{x_{inv}}1 \quad \boldsymbol{x_{inv}}2 \quad \boldsymbol{x_{load}} \quad \boldsymbol{x_{line}}]^T \tag{17}$$

$$\text{Output vector, } \boldsymbol{y} = [\Delta i_{oDQ1} \Delta i_{oDQ2} \Delta \omega_{PLL1} \Delta \omega_{PLL2}]^T \tag{18}$$

$$\text{Input vector, } \boldsymbol{u} = [\Delta v_{bD1} \Delta v_{bQ1} \Delta v_{bD2} \Delta v_{bQ2}]^T \tag{19}$$

Given a state perturbation of ΔA in state space, as; $\dot{x} = (A + \Delta A)x + Bu$

The perturbed eigen-triplets; i.e. eigenvalue $\Delta\lambda$, right eigenvectors $\Delta\emptyset_R$ and left eigenvectors $\Delta\emptyset_L$ of the perturbed system are given as;

$$(\emptyset_L + \Delta\emptyset_L)(A + \Delta A) = (\emptyset_L + \Delta\emptyset_L)(\lambda + \Delta\lambda) \tag{20}$$

$$(A + \Delta A)(\emptyset_R + \Delta\emptyset_R) = (\lambda + \Delta\lambda)(\emptyset_R + \Delta\emptyset_R) \tag{21}$$

The perturbations in state space modelling may affect the small signal stability and hence, needs to be considered while evaluating the complete state space modelling of the isolated microgrids [13,20]. While a small state perturbation, ΔA may not drastically unstabilize a stable system, but the stability of a marginally stable system or systems on the boundary, such as those with very small real-valued poles, may shift towards the right half of s-plane and, hence system may become unstable. This is discussed in section 7 in case 2.

4.2. Transfer function modelling

When the transfer function model of a system is given, its response to a specific input signal can easily be determined. Even mathematical computations are much easier when the system is in its Laplace transform domain. The current work utilizes the transfer function model for reduced order modelling so as to visualize the dominant poles in s-plane and develop reduced order response for any input signal. The overall transfer function model of autonomous microgrid (15,16) with outputs $i_{oD1}, i_{oQ1}, i_{oD2}, i_{oQ2} \omega_{PLL1}, \omega_{PLL2}$ and inputs $v_{bD1}, v_{bQ1}, v_{bD2}, v_{bQ2}$, is represented by 24 transfer functions from all inputs to outputs, given below;

$$G(s) = C(sI - A)^{-1}B = \begin{bmatrix} G_{11}(s) & G_{12}(s) & G_{21}(s) & G_{22}(s) \\ G_{31}(s) & G_{32}(s) & G_{13}(s) & G_{14}(s) \\ G_{23}(s) & G_{24}(s) & G_{33}(s) & G_{34}(s) \\ G_{41}(s) & G_{42}(s) & G_{51}(s) & G_{52}(s) \\ G_{61}(s) & G_{62}(s) & G_{43}(s) & G_{44}(s) \\ G_{53}(s) & G_{54}(s) & G_{63}(s) & G_{64}(s) \end{bmatrix} \tag{22}$$

where, $G_{ij}(s)$ is the transfer function between i^{th}output and j^{th} input,

$$G_{ij}(s) = \frac{N_{ij}(s)}{DC(s)} \tag{23}$$

$DC(s)$ is the 36th order common denominator, $N_{ij}(s)$ is the numerator of the transfer function $G_{ij}(s)$.

Out of this transfer function set of autonomous microgrid system, six are static gain due to no relationship between those pair of input-output signals. Table 3 tabulates all the 36 common poles of $DC(s)$ with their damping ratios and oscillatory frequencies obtained from their real and complex parts.

5. Optimal model order reduction

The processing speed and storage requirements of high-order systems, as well as their limitations in accuracy due to the high probability of errors in state matrices, makes the analysis computationally cumbersome. Parsimony principle defines the best approximant as "the one that accurately represents a transfer function with a minimum number of parameters." MOR facilitates the analysis of such systems by providing a near-to-good lower order replacement for its large order model [6].

The widely applied technique for MOR of LTI systems is Balanced Truncation approach, which originates from the controllability and observability gramians, W_C, W_O, respectively, as a solution of the Lypunov algebraic equation,

$$AW_C + W_C A^T = -BB^T \tag{24}$$

$$A^T W_O + W_O A = -C^T C \tag{25}$$

The "balanced" approach equalizes the gramians of the system through similarity transformation. The MOR is achieved by elimination of the smaller energy or uncontrollable-unobservable states. BT involves large matrix computations while analyzing larger power systems, for evaluating the controllability and observability of system. DC offset may occur while evaluating lower order approximations due to its inefficiency in following the original system's steady-state behaviour [4].

The method proposed in the paper to reduce the higher order microgrid model in (22) to its lower order counterpart is by using a combination of Dominant pole and Particle Swarm Optimisation technique. This proposed optimal reduction method takes the advantages of both the conventional dominant pole retention method and the most popular swarm intelligence technique of PSO. The principle of the dominant pole method is to retain the eigenvalues closes to the origin, hence retaining dominant time constants in the reduced model. Since the eliminated poles only impact the response at the beginning of a system, the retention of dominant poles gives the reduced model overall behaviour similar to the original one [9]. Considering

the reduced order transfer function model of (22) as

$$G_r(s) = C_r(sI - A_r)^{-1}B_r = \begin{bmatrix} G_{r11}(s) & G_{r12}(s) & G_{r21}(s) & G_{r22}(s) \\ G_{r31}(s) & G_{r32}(s) & G_{r13}(s) & G_{r14}(s) \\ G_{r23}(s) & G_{r24}(s) & G_{r33}(s) & G_{r34}(s) \\ G_{r41}(s) & G_{r42}(s) & G_{r51}(s) & G_{r52}(s) \\ G_{r61}(s) & G_{r62}(s) & G_{r43}(s) & G_{r44}(s) \\ G_{r53}(s) & G_{r54}(s) & G_{r63}(s) & G_{r64}(s) \end{bmatrix} \quad (26)$$

where, $G_{rij}(s)$ is the transfer function between output i^{th} output and j^{th} input with order "r" (r < 36);

$$G_{rij}(s) = \frac{N_{rij}(s)}{DC_r(s)} = \frac{b_{r-1}s^{r-1} + b_{r-2}s^{r-2} + \ldots + b_0}{a_r s^r + a_{r-1}s^{r-1} + \ldots + a_0} \quad (27)$$

$DC_r(s)$ is the r^{th} order common denominator,

$N_{rij}(s)$ is the numerator of the transfer function $G_{rij}(s)$.

The eigenvalues of the small signal model, highlighted in Table 3, are significantly closer to the origin as compared to other ones, and thus, are preserved in the reduced order approximant. This table also lists all the eigenvalues with mode nos. Thus, for a 9^{th} order reduced model, the modes taken from the original system are; oscillatory modes: 10,11,12,13 and a non-oscillatory mode: 16.

Now for optimal model order reduction, the numerator $N_{rij}(s)$ is to be determined such that the L_1 error norm between original and reduced order approximate system is minimum, i.e.

$$|error|_{step} = \int_0^\infty |g(t) - g_r(t)| \quad (28)$$

where, $g(t) = L^{-1}(G(s))$, is the step response of the original system; $g_r(t) = L^{-1}(G_r(s))$, is the step response of the reduced order system.

To fulfil the above requirement of minimum error, error minimization is achieved by determining the numerator polynomial, $N_{rij}(s)$ in (27) by utilising the evolutionary optimisation tool, Particle Swarm Optimization (PSO).

PSO is successfully used in optimization problems in every field of study [10,11]. It was developed by Eberhart and Kennedy in mid-1990s and adapted its behaviour from natural instances like a flock of birds, a shoal of fishes, etc. This tool results in higher flexibility and higher accuracy, which in turn helps to achieve the desired optimality with simple iterative programming. In the PSO algorithm, a collection of particles is placed randomly in the search space of the optimization problem. These particles move in a manner which is identical to movement of a flock of birds in nature in search of food and shelter. Then for a predefined number of iterations, the objective or fitness function of each particle is evaluated with their movements towards positions with better fitness. These movements are based on the particles own history of the best location in terms of fitness and best positions attained by other particles in the group, and some inertia from the current position with some random perturbations. Thus, the swarm obtains the most optimum solution to the fitness function in the problem space with a fixed number of particles working in synchronization [21]. The PSO update rule equations are given as;

$$v_{id}^{k+1} = wv_{id}^{k} + c_1 r_1^{k}(pbest_{id}^{k} - x_{id}^{k}) + c_2 r_2^{k}(gbest_{id}^{k} - x_{id}^{k}) \quad (29)$$

$$x_{id}^{k+1} = x_{id}^{k} + v_{id}^{k+1} \quad (30)$$

where, v_{id}^k and x_{id}^k represents velocity and position of the i^{th} particle (out of n particles) at d-dimension (out of D dimensions) in k^{th} iteration respectively.

$pbest_{id}^k$ and $gbest_{id}^k$ represents the personal best position and global best position (i.e. group's best) of the i^{th} particle (out of n particles) at d-dimension (out of D dimensions) in k^{th} iteration respectively.

w represents inertial weight attached to the particle's previously attained position; c_1, c_2 represent acceleration constants; r_1^k, r_2^k represent random numbers in the range of [0,1]. The flexibility, simple computations and high convergence rate in PSO based reduction technique yields an efficient lower order model which gives a good approximation to its full order original system.

6. Results and discussion

Uncertainty in system parameters, changes in operating point, fluctuations in the renewable energy resources connected as DGs as fluctuating irradiance, wind speed, etc. and load changes are some of the key reasons for state perturbation. It is worthy of mentioning that subject to these perturbations the stability analysis for full order as well as reduced order is indispensable.

The complete small signal modelling and order reduction of the microgrid system, in this paper, take into account the effect of uncertainty on the state space model, by considering a small perturbation of ΔA on the state matrix A linearized in the vicinity of a steady state operating point. The small signal model of an autonomous microgrid system consisting of two DERs, local loads and a connecting line is represented in state space by state space equations and output equations as in (15) and (16). The PLL angular frequency profile for perturbed and unperturbed microgrid system considered are given in Figure 4. The effect of state perturbations on autonomous micro grid system dynamics can be seen in Figure 5.

The dynamical response of v_{odq} and i_{odq} corresponding the system with and without perturb, are mentioned in Figure 5(c) and Figure 5(d). It is worthy to mention that the effect of the perturbation on the output

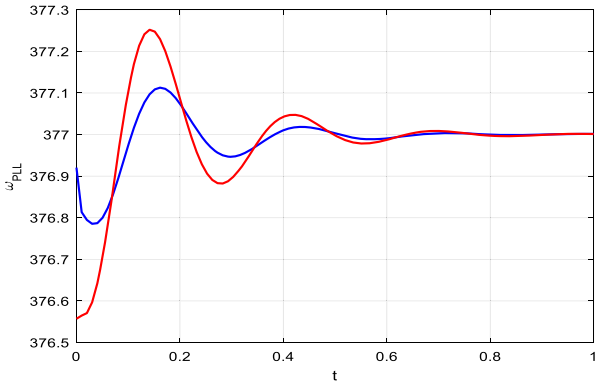

Figure 4. Measured frequency by PLL.

voltage and current profile almost tracks with little deviation in the initial period due to certain system uncertainties. After 0.5 s the tracking error is almost zero. Similar case is also visualized corresponding to other system behavioural quantities. Here convergence is almost achieved even earlier in the initial period.

The mathematical modelling with small signal analysis of the two inverter configuration as considered in this paper is represented by 36 state variables. In practical systems, the autonomous microgrid consists of a large number of DERs interconnected to meet the load requirements of an area. Thus, the small signal model tends to become computationally more complex. The order of higher order transfer functions is dimensionally simplified by utilizing the advantages of conventional dominant pole technique and PSO method. The error norm is used as the fitness function of particles in multiple iterations. The various parameters used in PSO algorithm are given in Table 1. The time responses of the full order and reduced order transfer functions by balanced truncation and proposed technique are given in Figure 6. The reduced order step response of $(\omega_{PLL1}(s))/(v_{bD2}(s))$ shows a steady state error by balanced reduction. The ISE and ITAE to step inputs, in the resulting reduced order transfer function model are given in Table A1 in the Appendix. The transfer functions from v_{bD1} to ω_{PLL1} , ω_{PLL2}, as seen from the table, give better-reduced order model by balanced truncation whereas, the other transfer functions give

Table 1. PSO Algorithm parameter values.

Parameter	Value
No. of generations	150
Swarm size	40
c_1,c_2	2.2,2.1
[w_{max},w_{min}]	[0.9,0.4]

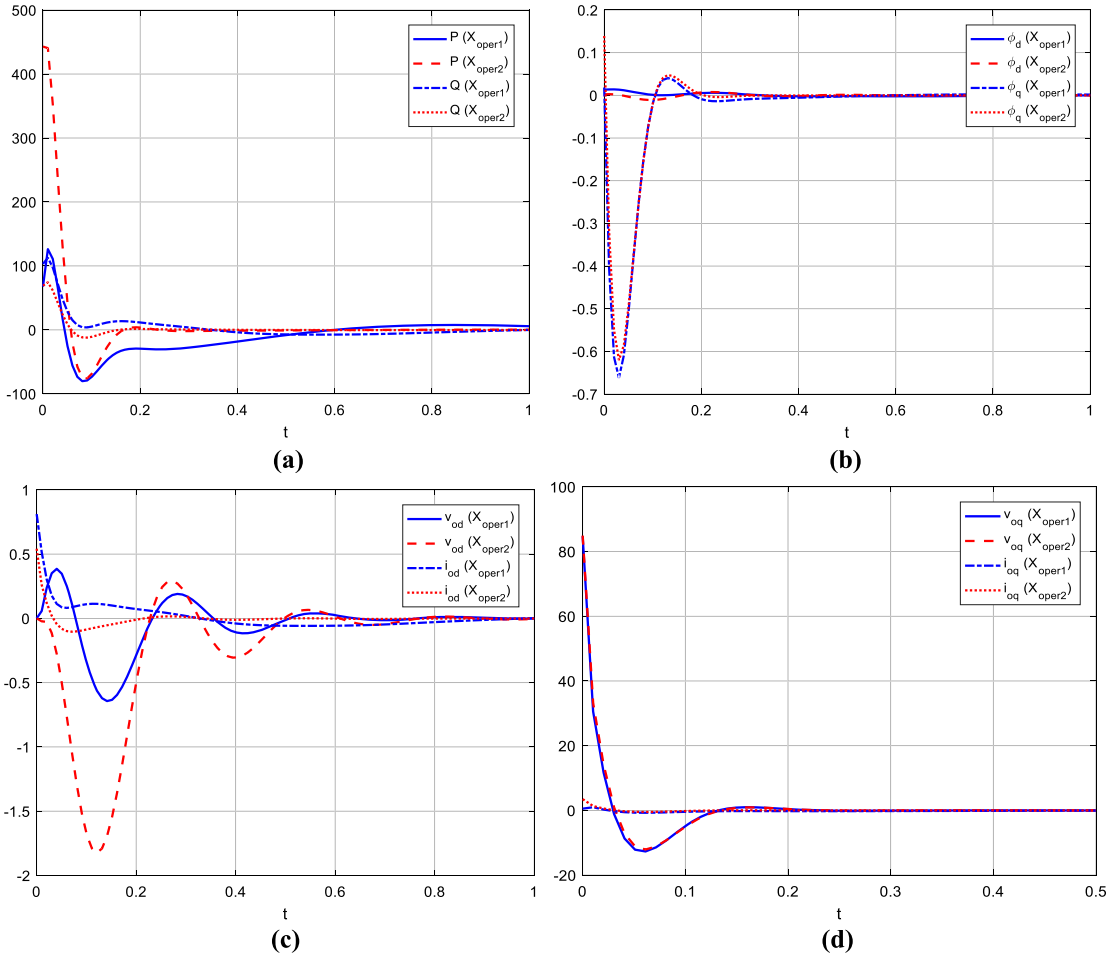

Figure 5. Autonomous Microgrid System Profile (blue line indicates unperturbed system and red line indicates perturbed system) (a) Active and reactive power, (b) $\emptyset_d$, $\emptyset_q$, (c) d-axis output current and voltage, (d) q-axis output current and voltage.

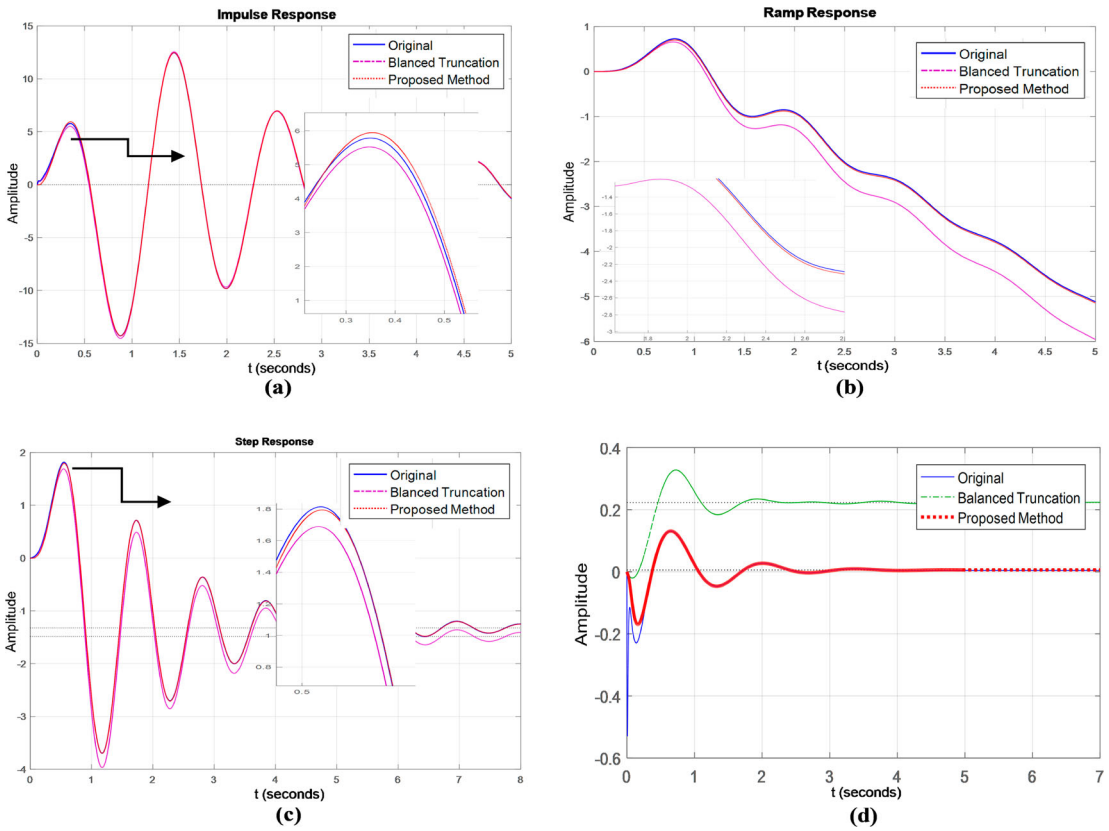

Figure 6. Time responses of full order and reduced order autonomous microgrid system. (a) Impulse response (b) Ramp response (c) Step response of $\frac{\omega_{PLL2}(s)}{v_{bQ1}(s)}$, (d) Step response of $\frac{\omega_{PLL1}(s)}{v_{bD2}(s)}$.

better results with the proposed method. This table also gives the errors in the reduction of the same system by balanced truncation approach.

The step, impulse and ramp responses of PLL angular frequency in Figure 6(a-c), show the dominance of the proposed method. Thus, the comparative analysis of these errors clearly indicates that the proposed method achieves better order reduction than the other method.

The changes in system dynamics due to perturbation (as in Figure 5), in the initial time period of system responses, makes it necessary to analyze the reduced order modelling of the perturbed system as well. Though for small changes in eigenvalues due to this perturbation, the deviations in reduced order transfer functions for the perturbed system will not be remarkable still their magnified impact can be seen in Figure 7. This figure shows that the proposed reduction method is not only good for the earlier small signal model of the microgrid, also gives a good approximation of perturbed microgrid systems as well.

The error norm (28) of the reduced order model with different standard inputs: Unit impulse input $\delta(t)$, unit step input $u(t)$. and unit ramp input $r(t)$; for both system without uncertainty and system with uncertainty, for some of the transfer functions of the system are given in Table 2. The impulse error norm is seen to be higher than the ramp and step error norm values.

The comparative analysis of the effects of MOR by the proposed method with BT, in the frequency

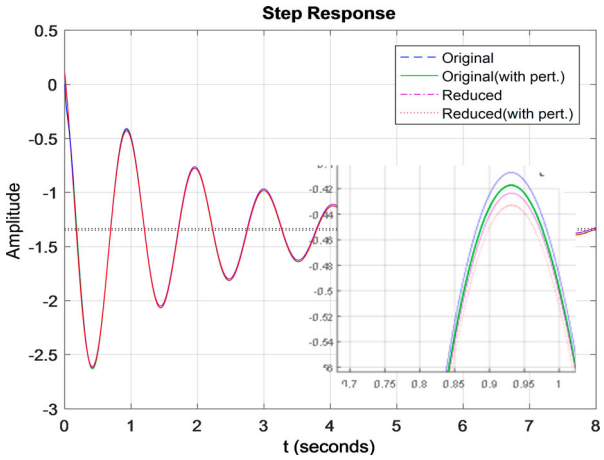

Figure 7. Model order reduction of the perturbed and unperturbed transfer function $\frac{i_{OQ1}(s)}{v_{bD1}(s)}$.

domain, in terms of gain margin (GM) and phase margin (PM) are given in Table A2 in Appendix. It is clearly seen that the GM and PM of the reduced order model by the proposed method are close to that of the original system. Therefore, it can be said that the results of reduced order modelling in the time domain are equally applicable in the frequency domain as the frequency domain features of the overall system remain close to that of the original system. Figure 8 represents the comparative analysis of the frequency response achieved by the proposed reduction technique as compared to the

Table 2. Impulse, step and ramp errors for microgrid transfer functions.

	ErrorNorm	$\frac{i_{OQ1}(s)}{v_{bD1}(s)}$	$\frac{\omega_{PLL1}(s)}{v_{bD1}(s)}$	$\frac{\omega_{PLL2}(s)}{v_{bD1}(s)}$	$\frac{i_{OQ1}(s)}{v_{bQ1}(s)}$	$\frac{\omega_{PLL1}(s)}{v_{bQ1}(s)}$	$\frac{\omega_{PLL2}(s)}{v_{bD2}(s)}$
Without Perturbation	$\|error\|_{\delta(t)}$	352.6298	674.4917	171.1216	83.1974	83.6241	48.1488
	$\|error\|_{u(t)}$	5.6677	5.8919	1.1341	2.0779	1.3624	1.7320
	$\|error\|_{r(t)}$	32.2833	33.6750	2.8756	0.3150	2.6041	6.6707
With Perturbation	$\|error\|_{\delta(t)}$	433.9358	732.2713	129.0163	15.6335	65.8360	29.3462
	$\|error\|_{u(t)}$	6.3115	2.5837	0.2793	0.0957	14.0356	0.5082
	$\|error\|_{r(t)}$	166.1388	29.6479	0.2750	0.4107	0.6040	4.9194

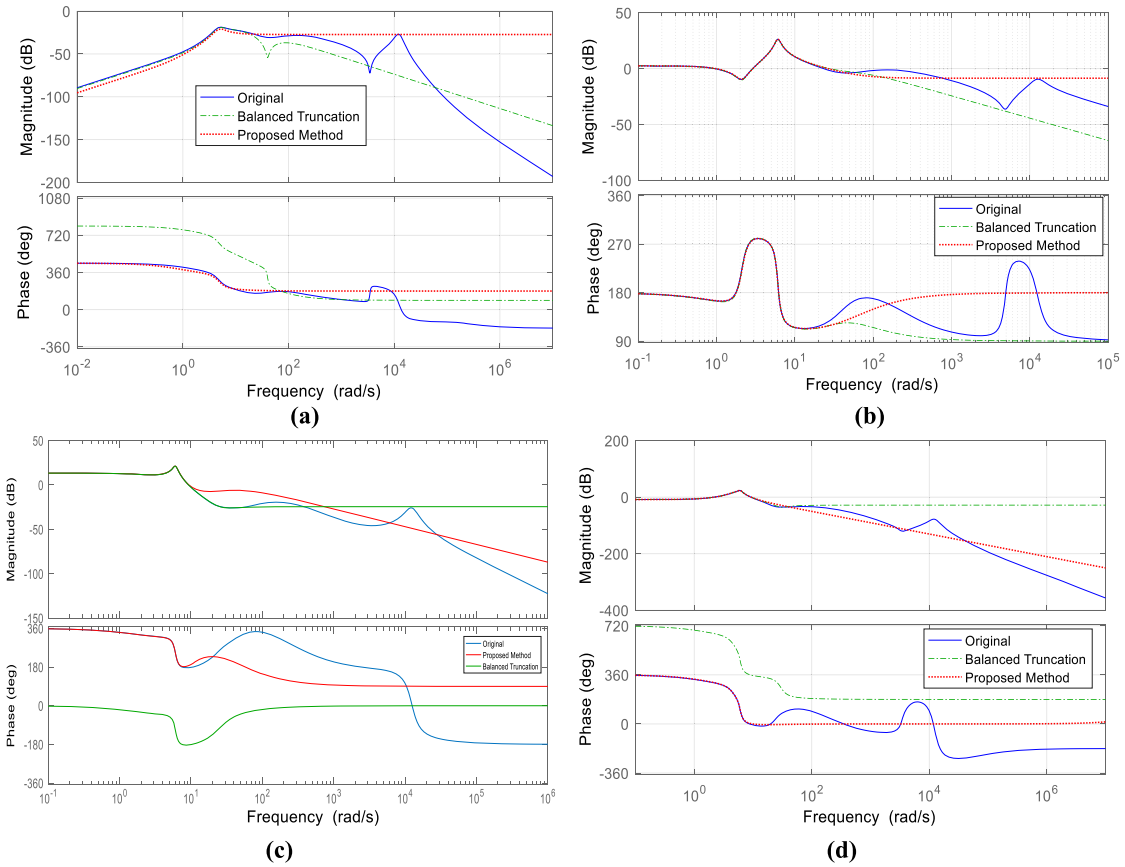

Figure 8. Bode plot of full order and reduced order transfer functions. (a) $\frac{i_{oQ1}(s)}{v_{bQ2}(s)}$, (b) $\frac{i_{oQ2}(s)}{v_{bQ1}(s)}$, (c) $\frac{\omega_{PLL1}(s)}{v_{bQ1}(s)}$, (d) $\frac{\omega_{PLL2}(s)}{v_{bQ1}(s)}$.

balanced truncation method. These magnitude plots of the optimal reduced order transfer function from input v_{bQ1} to output ω_{PLL12}, i_{oQ12}, give a better approximation to the full order model till frequencies of 100 rad/sec. The phase plots can be seen to give best approximants till 10 rad/sec.

The frequency analysis of the reduced order model of the perturbed system is not shown here as it will be much similar to that for the unperturbed system, which is been analyzed thoroughly in this paper. Stability and Eigenvalue analysis

A real eigenvalue corresponds to a non-oscillatory mode whereas, a complex eigenvalue is an oscillatory mode. The frequency of oscillation for oscillatory modes is obtained from the imaginary part of eigenvalues. The real part of eigenvalues gives the damping effect of that root on the system [22]. All the eigenvalues of the system in Table 3, have negative real parts. Thus, the necessary condition for small signal stability is fulfilled, i.e. $\sigma_i < 0$. The evaluation of the participation factor of a system is crucial to further enhance the stability. The participation matrix combines the right eigenvectors and left eigenvectors to measure the degree of association between all the state variables of the system and the system modes. The eigenvalue sensitivity is found out from this matrix, which gives the contribution or influence of a certain state variable to a certain mode [23].

As seen in Table 3, a total of 16 oscillatory/non-oscillatory modes are identified. The states representing output voltage and current in both d and q axis are observed to be highly oscillatory with frequencies of up to 1995Hz approximately. The lowest frequency of 0.005 Hz is in Mode 13 whose major contributors are active and reactive powers of the inverters. For eigenvalues with damping ratios from 0 to 1, i.e. underdamped dynamics, the settling time is inversely proportional and hence, lower ξ, corresponds to higher settling time.

Table 3. Eigenvalues, modes and mode contributor.

Eigen values	Real part ± j Imaginary part		Damping ratio, ξ	Damped frequency, f_i(Hz)	Mode		Highest Contributors
					Oscillatory	Non-Oscillatory	
3,4	−2500.5541	12528.6187	0.1958	1995.0030	1		v_{oq1}, i_{oq1}
5,6	−2499.7826	12526.5737	0.1957	1994.6773	2		v_{oq2}, i_{oq2}
7,8	−2321.4976	11784.7233	0.1933	1876.5483	3		v_{od1}, i_{od1}
9,10	−2317.9076	11780.4993	0.1930	1875.8757	4		v_{od2}, i_{od2}
11	−7912.5942	0	1			14	$v_{od1,f}$
12	−7903.6296	0	1			15	$v_{od2,f}$
1,2	−375	376.6084	0.7056	59.9695	5		i_{lineDQ}
13,14	−3333.3300	376.6084	0.9937	59.9695			$i_{loadDQ2}$
15,16	−1666.6667	376.6084	0.9754	59.9695			$i_{loadDQ1}$
19,20	−258.0320	64.1104	0.9705	10.2087	6		i_{ldq2}
17.18	−257.5532	60.9617	0.9731	9.7073	7		i_{ldq1}
21,22	−79.3639	16.5199	0.9790	2.6306	8		γ_{dq1}
23,24	−77.3698	19.2989	0.9703	3.0731	9		γ_{dq2}
25,26	−10.6101	7.8436	0.8041	1.2490	10		$\boldsymbol{\delta_2, \emptyset_{PLL2}}$
27,28	−0.4722	6.0420	0.0779	0.9621	11		$\emptyset_{\boldsymbol{dq}1}$
29,30	−1.2883	4.6232	0.2684	0.7362	12		$\emptyset_{\boldsymbol{dq}2}$
31	−2.1209	0	1			16	$\emptyset_{\boldsymbol{PLL}1}$
32,33	−50.2448	0.0308	0.9999	0.0049	13		$\boldsymbol{P_{12}, Q_{12}}$
34,35	−50.2515	0.0315	0.9999	0.0050			
36	0	0					δ_1

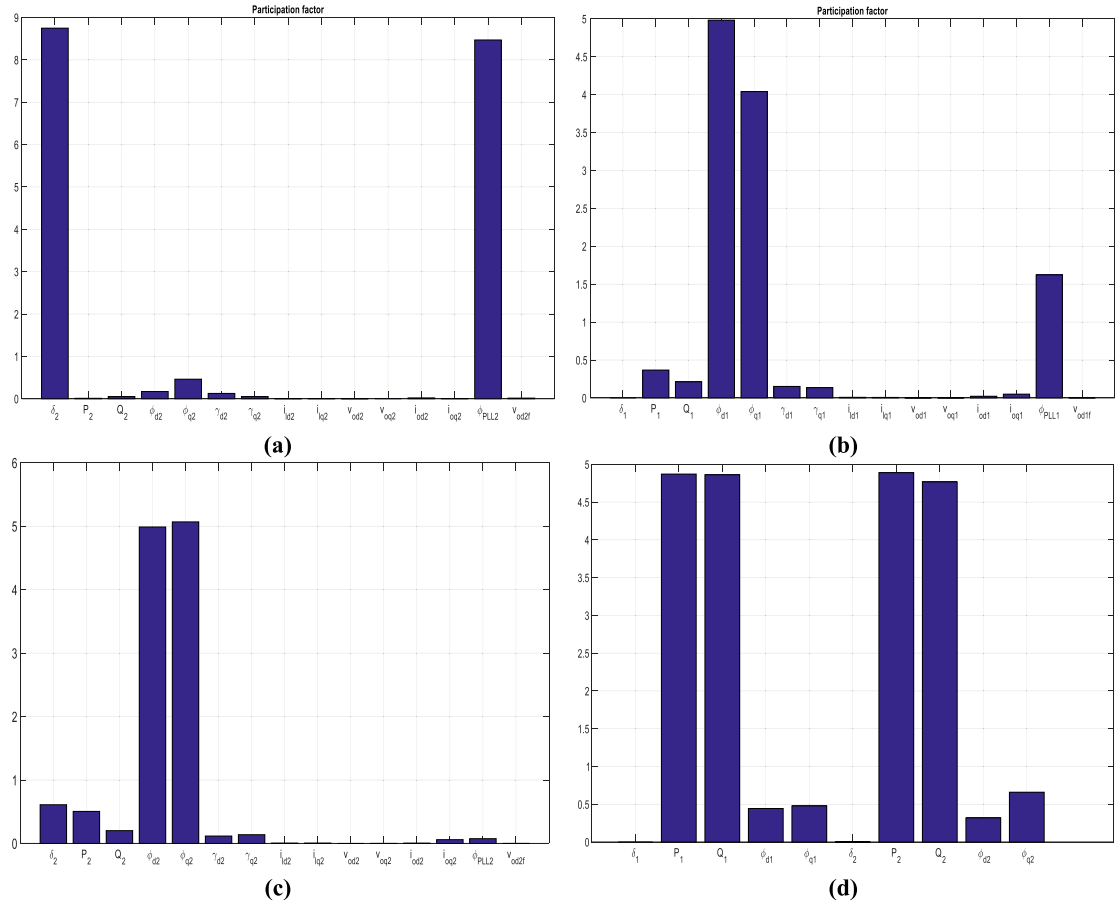

Figure 9. Bar graph representation of participation factors.(a) mode 10 (b) mode 11 (c) mode 12 (d) mode 13 (Reduced order oscillatory modes).

The damping ratios of the complex eigenvalues demonstrate the damped oscillations which die out and gives a stable overall system dynamics.

As system's reduced order model retains the eigenvalues with the smallest real part, thus, for a 9th order reduction, the corresponding modes that are considered are; mode 10, 11,12,13,16. Although the angle deviation of inverter 1 is considered as a slow state at the origin, it's small- signal response during both the transient and the steady state is zero. This state is thus ignored in the subsequent analysis when the reduced order system is being developed. Fast modes die out quickly in the system response, whereas, the slower mode's effect predominates throughout in response.

Table 4. Effect of perturbation on slow mode.

		λ + Δ λ		Damping ratio			Damped freq.(Hz)		
Indices	λ	CASE 1	CASE 2	ξ_{λ}	$\xi_{\lambda+\Delta\lambda}{}^{1}$	$\xi_{\lambda+\Delta\lambda}{}^{2}$	f_{λ}	$f_{\lambda+\Delta\lambda}{}^{1}$	$f_{\lambda+\Delta\lambda}{}^{2}$
25,26	−10.6101 ± j7.8436	−10.6204 ± j7.8297	−10.7297 ± j7.6884	0.804	0.805	0.813	1.249	1.247	1.224
27,28	−0.4722 ± j6.0420	−0.4732 ± j6.0419	0.0144 ± j4.6165	0.078	0.078	−0.003	0.962	0.962	0.735
29,30	−1.2883 ± j4.6232	−1.2785 ± j4.6296	−1.2521 ± j2.6654	0.268	0.266	0.425	0.736	0.737	0.424
31	−2.1209 ± j0	−2.1207 ± j0	−3.0613 ± j0	1	1	1			
32,33	−50.2448 ± j0.0308	−50.2515 ± j0.0235	−50.2532 ± j0.0130	0.999	0.999	0.999	0.005	0.004	0.002

Since these modes are slow with larger time constants as compared to the other modes, the overall reduced order response will be similar to the original system response, with negligible inaccuracies, mainly in the initial period of the response. The impact of the major state variables in these modes combined obtains the system response in reduced order. The quantitative analysis of the various state contributions in the retained oscillatory modes, i.e. Mode 10, 11, 12 and 13, are presented as a bar graph in Figure 9.

The state perturbation in the small signal model of the microgrid system causes the eigenvalues to deviate from their values calculated by linearization of the system about a steady state operating point. The small perturb in the eigenvalues will be insignificant for fast modes, as a change of 0.001 Hz will not change their dynamics much, but, for the slower modes, a change of 0.001 Hz will significantly increase the time constant of the system. Table 4 shows the effect of the perturbation on low-frequency eigenvalues. The changes in damping ratios and frequencies on these modes thereby changes the overall system response under perturbation. Significant parameter or load changes may even affect the stability of the overall system. Cases 1 and 2, in the table, demonstrate two different levels of uncertainty, wherein, the comparatively larger perturbation in case 2 makes the system unstable by the movement of the smallest real-valued mode toward the unstable region of s-plane. The state perturbation, in this case, results in a net negative damping in the overall system and frequencies as low as 0.002 Hz.

Due to small uncertainties considered in the system, the relative participation of states in different mode will not change and so, it is not evaluated again in this work.

7. Conclusion

An optimal reduced order model of the autonomous microgrid system is derived using the dominant pole retention and PSO technique. The poles nearest to origin are retained in the reduced order model, and the error between full order and reduced order model is minimized by adopting the PSO algorithm. The 36th order small signal model is reduced to a 9^{th} order approximation with high accuracies in time as well as frequency domain. The comparative analysis of the proposed order reduction method with that of balanced truncation method is also obtained by comparing the impulse, step and ramp responses; and bode plots obtained through both the methods. The eigenvalue analysis identifies the state variables of the original system, whose major influences are preserved in the reduced order model.

Considering a general perturbation in the system which may be due to parameter changes, changes in operating conditions etc., the effect of subsequent state perturbation on the full order and reduced order system have been critically analysed by considering their effects on the slower modes, as the deviations in the fast modes will not impact the system dynamical behaviour. Cases 1 and 2 in Table 4 demonstrate two different perturbations on the state space model wherein, the later one alters the system stability. The system dynamics of the derived 9^{th} order model of an autonomous microgrid is approximately same as that of its 36th full-order model, which has been proved by time and frequency domain analysis and, hence the optimal reduced order model can be used in all small signal analysis, stability requirements and other controller requirements.

Disclosure statement

No potential conflict of interest was reported by the authors.

Funding

This research did not receive any specific grant from funding agencies in the public, commercial, or not-for-profit sectors.

ORCID

Mudita Juneja http://orcid.org/0000-0002-5457-0127

References

[1] Yu K, Ai Q, Wang S, et al. Analysis and optimization of droop controller for microgid system based on small-signal dynamic model. IEEE Trans on Smart Grid. 2015;7(2):1–11. doi:10.1109/TSG.2015.2501316

[2] Rasheduzzaman M, Mueller JA, Kimball JW. An accurate small-signal model of inverter-dominated islanded microgrids using dq reference frame. IEEE J Emerg Sel Top Power Electron. 2014;2(4):1070–1080. doi:10.1109/JESTPE.2014.2338131.

[3] Fortuna L, Nunnari G, Gallo A. Model order reduction techniques with applications in electrical engineering. London: Springer; 1992. doi:10.1007/978-1-4471-3198-4

[4] Ghosh S, Senroy N. Balanced truncation approach to power system model order reduction. Electrical

Power Components and Systems. 2013;41(8):747–764. doi:10.1080/15325008.2013.769031.
[5] Luo L, Dhople SV. Spatiotemporal model reduction of inverter-based islanded microgrids. IEEE Trans Energy Conversion. 2014;29(4):823–832. doi:10.1109/TEC.2014.2348716.
[6] Rasheduzzaman M, Mueller JA, Kimball JW. Reduced-order small-signal model of microgrid systems. IEEE Trans Sustainable Energy. 2015;6(4):1292–1305. doi:10.1109/TSTE.2015.2433177.
[7] Kodra K, Zhong N, Gajic Z. Model order reduction of an islanded microgrid using singular perturbations. American Control Conference (ACC); Boston, USA; 2016; p. 3650–3655. doi:10.1109/ACC.2016.7525480
[8] Meng X, Qianggang VW, Zhou N, et al. Multi-time scale model order reduction and stability consistency certification of inverter-interfaced DG system in AC microgrid. Energies. 2018;11(1):254, doi:10.3390/en11010254.
[9] Davison EJ. A method for simplifying linear dynamic systems. IEEE Trans on Automatic Control. 1966;11(1):93–101. doi:10.1109/TAC.1966.1098264.
[10] Kennedy J, Eberhart R. Particle swarm optimization. Proc. IEEE Int. Conf. on Neural Networks. Perth, Australia; 1995; p. 1942–1948. doi:10.1109/ICNN.1995.488968
[11] Bai Q. Analysis of particle swarm optimization algorithm. Computer and Information Science CCSE. 2010;3:180–184. doi:10.5539/cis.v3n1p180
[12] Juneja M, Nagar SK. Comparative study of model order reduction using combination of PSO with conventional reduction techniques. Int. Conf. Indus. Instru. and Control; Pune, India; 2015; p. 406–411. doi:10.1109/IIC.2015.7150776
[13] Ma J, Wang X, Lan X. Small-signal stability analysis of microgrid based on perturbation theory. Power and Energy Eng. Conference; Asia-Pacific, China; 2012; p. 1–4. doi:10.1109/APPEEC.2012.6306946
[14] Hadisupadmo S, Hadiputro AN, Widyotriatmo A. A small signal state space model of inverter-based microgrid control on single phase AC power network. Internetworking Indonesia Journal. 2015;8(1):1–10. doi:10.1109/EPE.2015.7309119
[15] Pogaku N, Prodanovic M, Green TC. Modeling, analysis and testing of autonomous operation of an inverter-based microgrid. IEEE Trans Power Electronics. 2007;22(2):613–625. doi:10.1109/TPEL.2006.890003.
[16] Hassan MA, Abido MA. Optimal design of microgrids in autonomous and grid-connected modes using particle swarm optimization. IEEE Trans Power Electronics. 2011;26(3):755–769. doi:10.1109/TPEL.2010.2100101.
[17] Mohammadi FD, Vanashi HK, Feliachi A. State-space modelling, analysis, and distributed secondary frequency control of isolated microgrids. IEEE Trans Energy Conversion. 2018;33(1):155–165. doi:10.1109/TEC.2017.2757012.
[18] Bidram A, Nasirian V, Davoudi A, et al. Cooperative synchronization in distributed microgrid control. New York: Springer; 2017. pp. 7–43. doi:10.1007/978-3-319-50808-5
[19] Roubal J, Husek P, Stecha J. Linearization: students forget the operating point. IEEE Trans on Education. 2010;53(3):413–418. doi:10.1109/TE.2009.2026427.
[20] Li Y, Gao W, Muljadi E, et al. Novel approach for calculation and analysis of eigenvalues and eigenvectors in microgrids. Power Systems conference, Clemson University; South Carolina 2014; p. 1–5. doi:10.1109/PSC.2014.6808122
[21] Juneja M, Nagar SK. Particle swarm optimization algorithm and its parameters: a review. Int. conf. on Control, Computing, Comm. and Materials; Allahabad, India. 2016. doi:10.1109/ICCCCM.2016.7918233
[22] Kundur P, Balu NJ, Lauby MG. Power system stability and control. New York (NY): McGraw-Hill; 1994.
[23] Bottrell N. Small-signal analysis of active loads and large-signal analysis of faults in inverter interfaced microgrid applications. South Kensington, United Kingdom: Ph.D Thesis, Imperial College London; 2014.

Appendix

Table A1. ISE and ITAE for all transfer functions of autonomous microgrid.

	ISE		ITAE	
Transfer function	BT	Proposed	BT	Proposed
$i_{OD1}(s)/v_{bD1}(s)$	25.3748	22.4097	125.7981	106.4528
$i_{OQ1}(s)/v_{bD1}(s)$	7.1662	5.6677	1148.3734	53.9848
$i_{OD2}(s)/v_{bD1}(s)$	63.1841	3.0671	26.0544	22.9404
$i_{OQ2}(s)/v_{bD1}(s)$	9.3897	5.2964	32.8778	47.8019
$\omega_{PLL1}(s)/v_{bD1}(s)$	2.6144	5.8919	274.0537	194.6047
$\omega_{PLL2}(s)/v_{bD1}(s)$	0.3021	1.1341	166.1873	127.2240
$i_{OD1}(s)/v_{bQ1}(s)$	0.0782	0.0297	10.1155	7.2792
$i_{OQ1}(s)/v_{bQ1}(s)$	2.0955	2.0779	42.2261	86.1811
$i_{OD2}(s)/v_{bQ1}(s)$	0.7502	0.2190	53.0852	40.0971
$i_{OQ2}(s)/v_{bQ1}(s)$	1.8197	1.1118	78.3357	32.6199
$\omega_{PLL1}(s)/v_{bQ1}(s)$	11.7868	1.3624	1354.6428	175.0446
$\omega_{PLL2}(s)/v_{bQ1}(s)$	2.8359	1.7320	807.2399	184.1313
$i_{OQ1}(s)/v_{bD2}(s)$	1.9255	1.4104	3.0392	0.7847
$\omega_{PLL1}(s)/v_{bD2}(s)$	4.9850	4.3867	17.9070	2.2281
$\omega_{PLL2}(s)/v_{bD2}(s)$	26.9338	25.128	213.3036	63.8961
$i_{OQ1}(s)/v_{bQ2}(s)$	0.07350	0.0522	9.5347	0.6392
$\omega_{PLL1}(s)/v_{bQ2}(s)$	23.5205	1.4432	18.1278	1.4519
$\omega_{PLL2}(s)/v_{bQ2}(s)$	15.3154	13.4021	27.3498	11.7831

Table A2. Gain margin and phase margin of full order and reduced order autonomous microgrid.

	GM			PM (degrees)		
Transfer Function	Original	BT	Proposed	Original	BT	Proposed
$i_{OD1}(s)/v_{bD1}(s)$	0.82489	1.09702	0.82365	−23.62158	28.44517	–
$i_{OQ1}(s)/v_{bD1}(s)$	0.82774	0.84322	1.06409	25.94144	−25.48198	–
$i_{OD2}(s)/v_{bD1}(s)$	0.74987	0.70827	0.75015	−108.08955	−111.31156	−107.51302
$i_{OQ2}(s)/v_{bD1}(s)$	1.58496	–	2.12825	−2.76498	6.24817	−1.77988
$\omega_{PLL1}(s)/v_{bD1}(s)$	0.74269	0.75544	0.74818	−1.31455	−124.30003	−1.26627
$\omega_{PLL2}(s)/v_{bD1}(s)$	0.19983	0.20343	0.20787	−23.06178	−20.54071	−18.70413
$i_{OD1}(s)/v_{bQ1}(s)$	0.55514	0.55089	0.55715	45.37122	45.62369	45.18011
$i_{OQ1}(s)/v_{bQ1}(s)$	0.57881	0.52184	0.65434	37.93962	48.88312	40.54128
$i_{OD2}(s)/v_{bQ1}(s)$	0.35861	0.35861	0.35858	−161.72776	−161.41563	−159.97817
$i_{OQ2}(s)/v_{bQ1}(s)$	0.74939	0.74946	0.74931	−15.01546	−14.77873	−15.82536
$\omega_{PLL1}(s)/v_{bQ1}(s)$	0.09319	0.09360	0.09254	120.98238	121.89210	122.88868
$\omega_{PLL2}(s)/v_{bQ1}(s)$	0.75688	0.75551	0.75542	−73.20487	−72.74533	−73.65761
$i_{OQ1}(s)/v_{bD2}(s)$	4.36680	586.20700	9.68474	–	–	–
$\omega_{PLL1}(s)/v_{bD2}(s)$	1.47394	3.31899	2.51810	–	–	–
$\omega_{PLL2}(s)/v_{bD2}(s)$	16.78432	41.08055	1.25690	–	–	–
$i_{OQ1}(s)/v_{bQ2}(s)$	14.71627	13.23669	12.46060	–	–	–
$\omega_{PLL1}(s)/v_{bQ2}(s)$	0.31552	0.31545	0.31519	−1.46538	−145.41158	−13.17513
$\omega_{PLL2}(s)/v_{bQ2}(s)$	3.00617	3.32984	0.16855	−59.11295	−60.62443	−94.09749